8-1994

Performance of an Inertially Coupled, 3-Mode Gravitational-Wave Antenna Prototype

Linda E. Marchese
University of Rochester

Mark F. Bocko
University of Rochester

Guizhen Zhang
University of Rochester

Munawar Karim
Saint John Fisher College, mkarim@sjfc.edu

Publication Information

Marchese, Linda E.; Bocko, Mark F.; Zhang, Guizhen; and Karim, Munawar (1994). "Performance of an Inertially Coupled, 3-Mode Gravitational-Wave Antenna Prototype." *Review of Scientific Instruments* 65.8, 2627-2634.

Performance of an Inertially Coupled, 3-Mode Gravitational-Wave Antenna Prototype

Abstract

A prototype three-mode gravitational wave antenna which employs a two-mode torsional transducer has been constructed and tested. For the torsional transducer the coupling from one stage to the next is via inertial forces, whereas in a conventional transducer the stage-to-stage coupling is proportional to the relative displacements via the springs. Experiments with our antenna-torsional transducer prototype demonstrate a maximum antenna bandwidth of 260 Hz (29% of the antenna resonant frequency of 900 Hz) and a mechanical amplification factor of 40. A mathematical model for the three-mode antenna has been developed and predictions of the system transfer functions and transient response are in close agreement with the measurements. Through the optimization of the transducer parameters we find that maximum fractional antenna bandwidths near 30% may be simultaneously achieved with mechanical amplification factors of 100 or more. Furthermore, the torsional transducer has a larger mechanical gain-antenna bandwidth product than a linear transducer with similar masses.

Keywords

Resonant-Mass, Radiation, Detectors

Disciplines

Physics

Performance of an inertially coupled, three-mode gravitational wave antenna prototype

Linda E. Marchese, Mark F. Bocko, and Guizhen Zhang
Department of Electrical Engineering, University of Rochester, Rochester, New York 14627

Munawar Karim
Department of Physics, St. John Fischer College, Rochester, New York 14618

(Received 29 March 1994 accepted for publication 5 May 1994)

A prototype three-mode gravitational wave antenna which employs a two-mode torsional transducer has been constructed and tested. For the torsional transducer the coupling from one stage to the next is via inertial forces, whereas in a conventional transducer the stage-to-stage coupling is proportional to the relative displacements via the springs. Experiments with our antenna-torsional transducer prototype demonstrate a maximum antenna bandwidth of 260 Hz (29% of the antenna resonant frequency of 900 Hz) and a mechanical amplification factor of 40. A mathematical model for the three-mode antenna has been developed and predictions of the system transfer functions and transient response are in close agreement with the measurements. Through the optimization of the transducer parameters we find that maximum fractional antenna bandwidths near 30% may be simultaneously achieved with mechanical amplification factors of 100 or more. Furthermore, the torsional transducer has a larger mechanical gain-antenna bandwidth product than a linear transducer with similar masses.

I. INTRODUCTION

The search for gravitational waves from astrophysical sources is continuing with the development of the third generation of Weber-bar gravitational radiation antennae. The first generation of room-temperature detectors achieved a gravitational wave strain sensitivity h near 10^{-17} and no confirmed events were recorded.[1] In 1981 Stanford University operated the first second generation gravitational wave antenna[2] and at present, several second generation gravitational wave antennae with strain sensitivities h approaching 10^{-19} are in operation.[3] Such detectors are constructed of large aluminum cylinders cooled to liquid-helium temperature (4.2 K) and instrumented with superconducting quantum interference device (SQUID) based electromechanical transduction systems. The approaching third generation detectors will employ improvements such as the use of larger cross-sectional spherical antennae, millikelvin operation, and nearly quantum limited transduction systems which will yield sensitivities surpassing $h \sim 10^{-21}$ which will almost certainly assure the detection of astrophysical sources of gravitational waves and found a new branch of astronomy.

One improvement likely in the third generation of detectors will come by implementing multi-mechanical mode transducers. In the present second generation of gravitational wave antennae an electromechanical transducer which is mechanically resonant at the frequency of the antenna is employed, and the antenna-transducer system displays two coupled mechanical modes. Third generation detectors which implement transducers with more than one resonant mode will benefit from higher mechanical amplification, stronger electromechanical coupling and larger detection bandwidths. There have been a number of papers[4–8] on multimechanical mode transducers for a gravitational wave antenna. Price and Bassan have showed that, for systems with more than three modes, the increase in bandwidth is slight as the number of modes is increased.[4,7] Consequently, it seems reasonable to concentrate on a three-mode system composed of a massive antenna and a two-mode transducer.

In this paper we discuss the development of a prototype three-mode gravitational wave detector which is composed of a dumbbell-shaped antenna and a two mechanical-mode transducer composed of two coupled torsional resonators. The mechanical element of most transducers in operation or under development is a mass loaded diaphragm which is equivalent to a linear mass, spring system. The innovation of using a torsional transducer, which is a rectangular prism supported by torsion springs offset from the prism's center of mass, offers a number of advantages. The first advantage, and the original motivation for this work, is that this transducer geometry allows coupling to the surface of the mechanical element of the transducer in a push–pull capacitive bridge circuit with both capacitors in one plane, making it much easier to fabricate and electrically tune the transducer readout circuit. In our modeling and experimentation with torsional transducers we have discovered the further advantage of this design over linear transducers which is a larger antenna bandwidth for given transducer masses. We have also found that the torsional transducer is very convenient to fabricate and mechanically tune.

In the following section we give a description of the prototype antenna-transducer system. We then present a simple model of the system and use it to determine the predicted bandwidth and mechanical amplification of the system. In the following section we describe the experimental results with our three-mode prototype antenna and in the final section, we discuss the sensitivity and optimization of a three-mode antenna employing the two-mode torsional transducer.

 0034-6748/94/65(8)/2627/8/$6.00

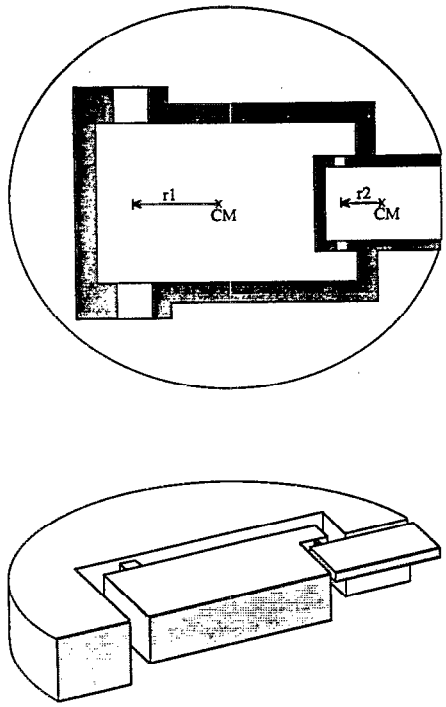

FIG. 1. The two-mode torsional transducer viewed from top and in cross section.

II. ANTENNA DESCRIPTION AND FABRICATION

The transducer, fabricated from a 15.2-cm-diam by a 3.8-cm-thick disk of aluminum 6061, is bolted to the end face of a dumbbell-shaped Al 6061 bar of mass 25 kg and length 0.61 m with the resonant frequency of its longitudinal mode at 900 Hz. The torsional resonators comprising the transducer are two rectangular prisms supported by off-center torsion springs with the second, smaller prism being attached near the end of the first (see Fig. 1). Both torsional resonators are tuned to the bar frequency of 900 Hz. The masses of the rectangular prisms are 0.343 and 0.0086 kg, respectively. The torsion spring supports are offset from the center of mass of each rectangular prism so that the translational motion of the transducer perpendicular to the disk face results in excitation of the torsional modes.

We developed a semiempirical, yet highly effective, method for fabricating the transducer. For optimal coupling it is required that the resonant frequency of both uncoupled torsional resonators be tuned to the bar frequency. It is time consuming, and not always sufficiently accurate, to make frequency predictions through calculation or computer modeling so we developed a semiempirical iterative method. We started by making an approximate calculation of the required torsion spring dimensions and the fabrication commenced by machining the smaller torsional resonator from the transducer blank. When the spring dimensions of the small torsional resonator were close to the target value we measured the resonant frequency *in situ*, i.e., with the transducer mounted to the milling machine being used for the machining process. An accurate measurement of the resonant frequency could be made by simply tapping the transducer, detecting the tone with a microphone and measuring the

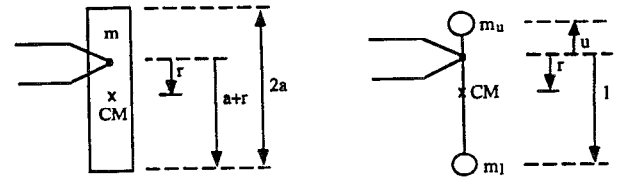

FIG. 2. The extended body model of a single torsional resonator is shown on the left and its lumped mass equivalent is shown on the right.

frequency on a Fourier transform spectrum analyzer. In this way the frequency of the small resonator could be tuned to within 1 Hz of the target value. After the completion of this stage, the machining of the second, larger, torsional resonator was begun in a similar iterative procedure. However, as the target frequency of the larger torsional resonator was approached, the mechanical coupling between the two torsional resonators gave rise to two coupled modes. The frequency splitting between the two normal modes reaches a minimum when the two uncoupled frequencies are tuned to each other. Therefore we monitored the frequency difference between the two normal modes and machined the springs of the larger torsional resonator until the minimum mode splitting was observed which indicated that the two uncoupled frequencies were properly tuned to one another and to the antenna.

III. MODEL

In this section we describe the torsional resonator model which we used to predict the mechanical behavior of the antenna, two-mode torsional transducer system. We begin by developing the model of a single torsional resonator. The displacement which we choose to define the motion of the resonator is that of the end of the rectangular prism furthest from the spring support. If the resonator were capacitively or inductively coupled to a readout circuit and the active area of the capacitor or inductor were distributed over some portion of the rectangular prism face, it would be straightforward to redefine the effective displacement in terms of our chosen displacement. The model is shown in Fig. 2. A rectangular prism of mass m and length $2a$ supported by a torsional spring located a distance r from the center of mass, can be represented as a rigid massless rod with two masses, m_u and m_l, located distances u and l, respectively, from the pivot point. The rod is supported by a torsional spring also located a distance r from the center of mass of the idealized system.

We place the following two constraints on the model: First, the total mass must be equal to the physical mass of the prism ($m=m_u+m_l$) and second, the distance from the pivot point to m_l must be equal to the distance between the pivot point and the far end of the prism, $l=a+r$. This constraint insures that the displacement of m_l in the model is the same as the displacement of the end of the rectangular prism.

Using the above constrains we equate the moments of inertia of the rectangular prism and our ball and stick model to find the model parameters in terms of the parameters of the physical transducer. The relationships are the following:

$$l=a+r, \quad u=\tfrac{1}{3}a-r, \quad m_l=\tfrac{1}{4}m, \quad m_u=\tfrac{3}{4}m. \tag{1}$$

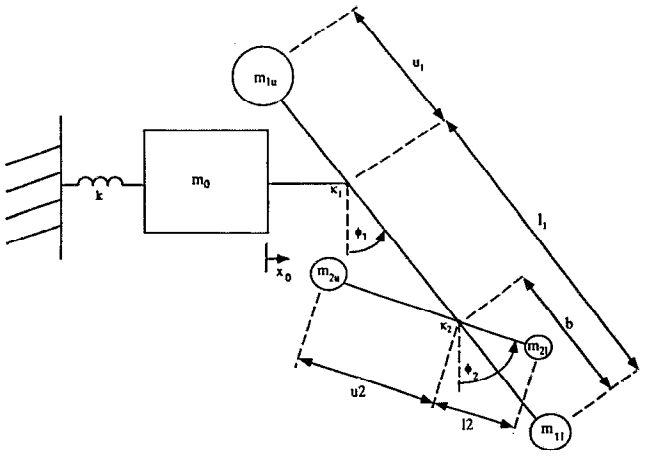

FIG. 3. Model of the three-mode gravitational wave antenna consisting of a bar, represented by a mass on a spring, and a two-stage torsional resonator.

Figure 3 illustrates the model of the antenna and a two-mode torsional transducer. The antenna, which in our case is a dumbbell-shaped bar, is represented as a linear oscillator of mass m_0 on a spring with stiffness k. The total masses of the first and second torsional resonators are m_1 and m_2, respectively. Located a distance u_1 from the pivot point of the first torsional resonator is m_{1u} and m_{1l} is located a distance l_1 on the opposite side of the same pivot. We define similarly the corresponding parameters for the second torsional resonator;

TABLE I. Displacements, relative to the laboratory coordinate system, of the masses comprising the three-mode antenna.

Mass	Displacement
m_0	x_0
m_{1u}	$x_0-u_1\phi_1$
m_{1l}	$x_0+l_1\phi_1$
m_{2u}	$x_0+(l_1-b)\phi_1-u_2\phi_2$
m_{2l}	$x_0(l_1-b)\phi_1+l_2\phi_2$

m_{2u}, u_2, m_2, and l_2. The positions of the torsional springs relative to the center of mass of the first and second resonators are r_1 and r_2, respectively (not shown on figure), and b is the distance from m_{1l} to the attachment point of the first torsional resonator to the second. The torsional spring constants are given by κ_1 and κ_2.

The equations of motion were found in a coordinate system fixed to the support of m_0, the laboratory coordinate system. We use ϕ_1 and ϕ_2 to represent the angular displacements of the two torsional oscillators from the vertical. The displacements of the various masses are defined in Table I. Using these definitions we found the Lagrangian for the system and the corresponding equations of motion following the usual procedure. Using the following definitions $x_1=l_1\phi_1$, $x_2=l_2\phi_2$, $\omega_0=(k_0/m_0)^{1/2}$, $\omega_1=(\kappa_1/m_1l_l^2)^{1/2}$, $\omega_2=(\kappa 2/m_2l_2^2)^{1/2}$, and $v_j=dx_j/dt(j=0,1,2)$ we can write the system equations, in the small angle approximation, as the following matrix equation:

$$
\begin{bmatrix}
1 & 0 & 0 & 0 & 0 & 0 \\
0 & 1+\dfrac{m_1+m_2}{m_0} & 0 & \dfrac{m_{1l}-m_{1u}\left(\dfrac{u_1}{l_1}\right)+m_2\left(\dfrac{l_1-b}{l_1}\right)}{m_0} & 0 & \dfrac{m_{2l}-m_{2u}\left(\dfrac{u_2}{l_2}\right)}{m_0} \\
0 & 0 & 1 & 0 & 0 & 0 \\
0 & \dfrac{l_1[m_{1l}l_1-m_{1u}u_1+(l_1-b)m_2]}{m_{1l}l_1^2+m_{1u}u_1^2} & 0 & 1+\dfrac{(l_1-b)^2m_2}{m_{1l}l_1^2+m_{1u}u_1^2} & 0 & \dfrac{l_1(l_1-b)(m_{2l}l_2-m_{2u}u_2)}{l_2 \quad m_{1l}l_1^2+m_{1u}u_1^2} \\
0 & 0 & 0 & 0 & 1 & 0 \\
0 & \dfrac{l_2(m_{2l}l_2-m_{2u}u_2)}{m_{2l}l_2^2+m_{2u}u_2^2} & 0 & \dfrac{l_2(l_1-b)(m_{2l}l_2-m_{2u}u_2)}{l_1 \quad m_{2l}l_2^2+m_{2u}u_2^2} & 0 & 1
\end{bmatrix}
\begin{bmatrix} \dot{x}_0 \\ \dot{v}_0 \\ \dot{x}_1 \\ \dot{v}_1 \\ \dot{x}_2 \\ \dot{v}_2 \end{bmatrix}
$$

$$
=\begin{bmatrix}
0 & 1 & 0 & 0 & 0 & 0 \\
-\omega_0^2 & 0 & 0 & 0 & 0 & 0 \\
0 & 0 & 0 & 1 & 0 & 0 \\
0 & 0 & -\omega_1^2-\omega_2^2\left(\dfrac{m_{1l}l_2^2+m_{2u}u_2^2}{m_{1l}l_1^2+m_{1u}u_1^2}\right) & 0 & \omega_2^2\left(\dfrac{m_{2l}l_2^2+m_{2u}u_2^2}{m_{1l}l_1^2+m_{1u}u_1^2}\right)\left(\dfrac{l_1}{l_2}\right) & 0 \\
0 & 0 & 0 & 0 & 0 & 1 \\
0 & 0 & \omega_2^2\left(\dfrac{m_{2l}l_2^2+m_{2u}u_2^2}{m_{1l}l_1^2+m_{1u}u_1^2}\right)\left(\dfrac{l_2}{l_1}\right) & 0 & -\omega_2^2 & 0
\end{bmatrix}
\begin{bmatrix} x_0 \\ v_0 \\ x_1 \\ v_1 \\ x_2 \\ v_2 \end{bmatrix}. \qquad (2)
$$

For comparison we include the equivalent system of equations for a conventional mass-linear spring three-mode trans-

ducer. In this model, which is a good representation of the mechanical elements of existing liner transducers, the effective mass of each transducer stage is connected to the preceeding stage by a linear spring as shown in Fig. 4. The equations are the following:

$$\begin{bmatrix} 1 & 0 & 0 & 0 & 0 & 0 \\ 0 & 1 & 0 & 0 & 0 & 0 \\ 0 & 0 & 1 & 0 & 0 & 0 \\ 0 & 0 & 0 & 1 & 0 & 0 \\ 0 & 0 & 0 & 0 & 1 & 0 \\ 0 & 0 & 0 & 0 & 0 & 1 \end{bmatrix} \begin{bmatrix} \dot{x}_0 \\ \dot{v}_0 \\ \dot{x}_1 \\ \dot{v}_1 \\ \dot{x}_2 \\ \dot{v}_2 \end{bmatrix} = \begin{bmatrix} 0 & 1 & 0 & 0 & 0 & 0 \\ -\omega_0^2 - \dfrac{m_1}{m_0}\omega_1^2 & 0 & \omega_1^2 \dfrac{m_1}{m_0} & 0 & 0 & 0 \\ 0 & 0 & 0 & 1 & 0 & 0 \\ \omega_1 & 0 & -\omega_1^2 - \omega_2^2 \dfrac{m_2}{m_1} & 0 & \omega_2 \dfrac{m_2}{m_1} & 0 \\ 0 & 0 & 0 & 0 & 0 & 1 \\ 0 & 0 & \omega_2^2 & 0 & -\omega_2^2 & 0 \end{bmatrix} \begin{bmatrix} x_0 \\ v_0 \\ x_1 \\ v_1 \\ x_2 \\ v_2 \end{bmatrix}. \tag{3}$$

The fundamental difference between the torsional transducer and the linear spring transducer is that the coupling between successive stages is through the inertia terms in the torsional system and the spring terms in the linear system. Therefore the two types of transducers are fundamentally dynamically different and it is not possible to represent the torsional system as an equivalent linear transducer. Therefore, it should not come as a surprise that the mechanical amplification and bandwidth are different for the torsional and linear-spring systems.

Equation (2) was solved on a computer to predict both the steady-state response of the torsional transducer system and the transient response. In the steady-state analysis Eq. (2) was Fourier transformed, the transfer function between the measurable quantity and the force acting on the antenna was computed. The variable which we adopted as the observable quantity is the displacement of the end of the last torsional resonator relative to the antenna end face. In practice the plates of a capacitor are attached, one to the last torsional resonator and the other to the antenna end face, so that the gap of the capacitor is modulated by the output observable $(1-b/l_1)x_1+x_2$. We plot the transfer function so fined in Fig. 5(a). For the measured values of the various physical parameters of our prototype transducer (shown in Table II) the three normal modes of the system are predicted to appear at ~767, 898, and 1027 Hz. We define the maximum bandwidth of the multimode antenna as the frequency difference between the extremal modes. Therefore, we have a theoretical value of 260 Hz for the maximum bandwidth of the model system.

The equations of motion were also solved numerically in the time domain to examine the transient response of the system to an impulsive force, such as a gravitational wave burst acting on the antenna. In the transient simulation program all resonant frequencies ω_j are normalized to the antenna frequency and an impulsive force which acts on the antenna at $t=0$ is assumed. Further normalization is per-

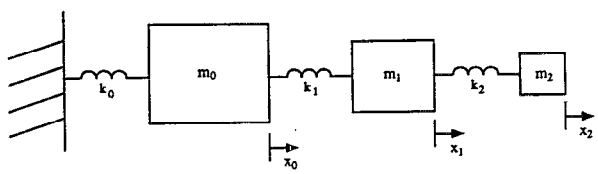

FIG. 4. Model of a three-mode gravitational wave antenna consisting of a bar and a two-stage liner transducer.

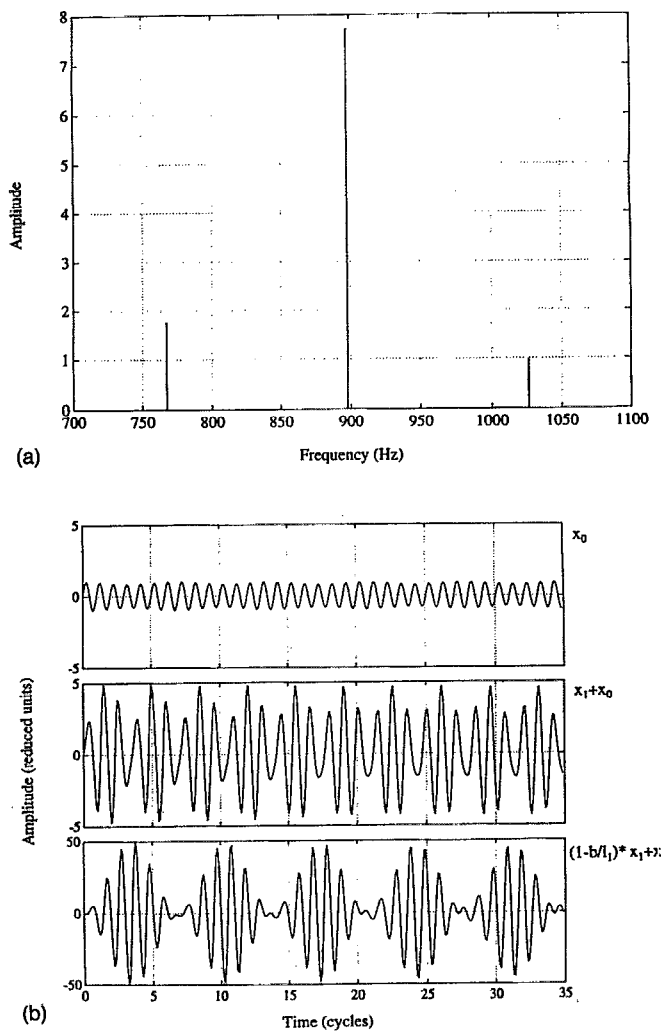

FIG. 5. (a) Predicted mechanical transfer function for the three-mode antenna with a two-stage torsional transducer. The mechanical parameters used to make the prediction are those of the prototype transducer we constructed. (b) Predicted transient response of the three-mode torsional system for an impulse applied to the bar.

TABLE II. Prototype two-mode torsional transducer parameters and optimum parameter values determined through simulations.

Parameter	Prototype value	Optimum value
m_0	25 kg	25 kg
$m_1=m_{1l}+m_{1u}$	0.343 kg	0.5 kg
$m_2=m_{2l}+m_{2u}$	0.0086 kg	0.0025 kg
a_1	4.500 cm	4.500 cm
r_1	2.600 cm	2.970 cm
l_1	7.100 cm	7.470 cm
a_2	2.075 cm	0.900 cm
r_2	1.200 cm	0.590 cm
l_2	3.275 cm	1.490 cm
b	−0.765 cm	−0.450 cm

formed to make the maximum amplitude of the antenna x_0 equal to unity. Furthermore, the time axis on the predicted transient response is in units of the number of cycles of oscillation at the antenna frequency. Figure 5(b) is a plot of the predicted transient response of the antenna and the two torsional oscillators. As previously stated, the maximum amplitude of the antenna end face is defined to be one displacement unit. The mechanical amplification of the first torsional resonator is ~5 and the smaller torsional resonator reaches a maximum amplitude of ~50 times the antenna end-face displacement. We also note that the rise time for the second torsional resonator to reach it's maximum amplitude is ~3.5 oscillation cycles.

Finally, in this section we compare the transient behavior of a three-mode system to a two-mode torsional transducer system with the same mechanical amplification factor of 50; see Fig. 6 for a plot of the two-mode system transient response. We see that the maximum amplitude of the single torsional resonator in the two-mode system is reached for after ~17 cycles so the three-mode system has a rise time approximately five times faster than the two-mode system. The maximum bandwidth of the three-mode system is also therefore correspondingly larger.

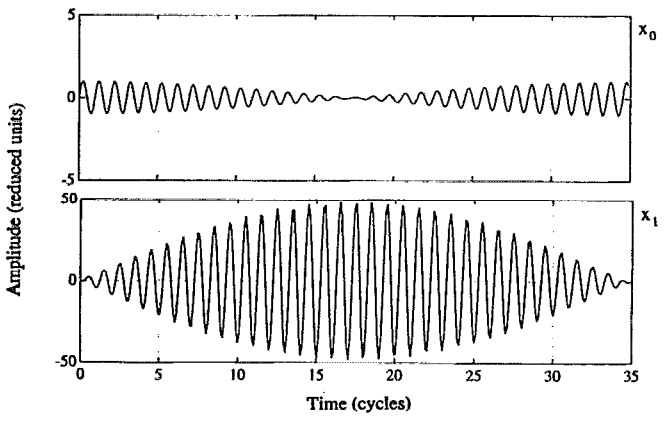

FIG. 6. Predicted transient response of a two-mode system composed of a bar and a single torsional transducer. The energy transfer time is ~17 oscillation cycles to reach the same mechanical amplification factor of 50 of the three-mode transducer.

IV. EXPERIMENTAL RESULTS

Our prototype three-mode gravitational wave antenna consisted of a dumbbell-shaped bar mounted vertically with the double torsional resonator bolted to the top of the bar. The transducer readout circuit was a dc biased capacitor microphone circuit. The top capacitor plate was a 2.1 cm^2 by 2.8 cm^2 plate covering approximately half of the area of the second torsional resonator. The capacitor gap was 0.92 mm giving a capacitance of 58 pF. We monitored the motion of the bar end face and larger torsional resonator with commercially available accelerometers. The accelerometer each had a mass of 5.2 g, which was not large enough to significantly affect the frequencies of the bar or the larger torsional resonator. The outputs from the accelerometers and the capacitor readout were recorded and plotted on a chart recorder which could capture three channels simultaneously. Therefore, we were able to observe the transient behavior of each harmonic oscillator after the application of an impulsive force to the antenna. The output of the capacitor circuit was calibrated against a factory calibrated accelerometer; thus we were able to simultaneously make calibrated displacement measurements of all three resonators comprising the antenna system. We also could determine the transfer function of the antenna by applying a white-noise driving force to the bar through a piezoelectric strain gauge and measuring the spectrum of the smaller torsional oscillator displacement signal from the capacitor circuit.

Figure 7(a) is a plot of the measured transfer function of the bar-torsional transducer system. The three modes of the system are observed at 770, 889, and 1029 Hz and the relative amplitudes closely correspond to the predicted transfer function in Fig. 5(a). Furthermore, each of the observed mode frequencies is within 3 Hz of the predicted frequencies. The predicted mode frequencies depend weakly upon the parameter b, which defines the location of the point of attachment of the smaller torsional resonator to the larger resonator and it was difficult to measure b accurately due to the finite size of the torsion springs. The value of b we chose for the simulation lay within the range inferred from our measurements and gave close agreement between the predicted and observed transfer functions.

The measured transient response of the three resonators is shown in Fig. 7(b). These measurements were made by applying an impulsive force to the bar. The rise time for energy transfer to the smaller torsional resonator is 4.6 ms (or 3.5 cycles) in close agreement with the model. The measured mechanical amplification, i.e., the ratio of the displacement of the end of the smaller torsional resonator to the displacement of the bar end face, was 40. The predicted amplification was ~50 but we believe that uncertainties in the calibration of the capacitor readout circuit and ambiguities in the model parameters used in the calculation due to the extended size of the torsion springs can account for the difference between the observed and predicted transient response.

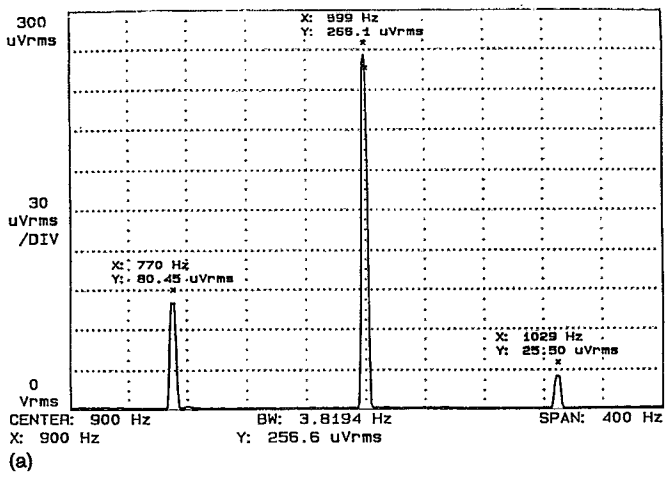

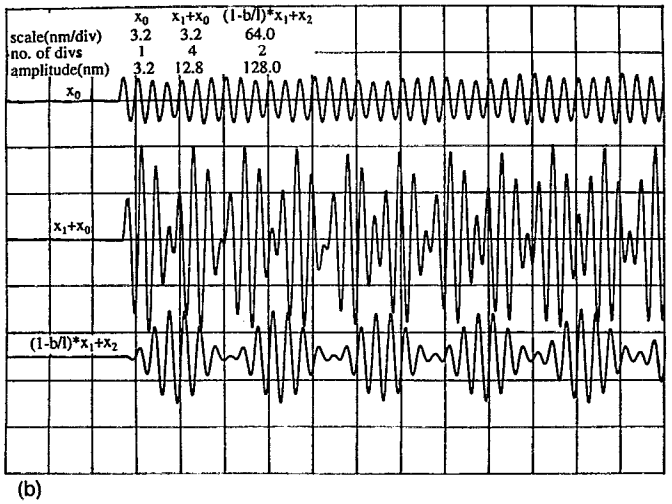

FIG. 7. (a) Measured transfer function of the prototype three-mode torsional transducer system. (b) Measured transient response of the three-mode torsional transducer.

V. OPTIMIZATION OF THE TORSIONAL TRANSDUCER AND COMPARISON TO LINEAR SPRING-MASS TRANSDUCERS

The transducer described above was fabricated prior to the completion of our theoretical model and thus, not surprisingly, the dimensions of the transducer were not optimized to give the maximum mechanical gain. For a linear transducer when the mass ratio between successive stages is a constant μ, where $\mu=m_{i+1}/m_i(i=0,1,2,3...)$ the transducer is optimized,[5,6,8] i.e., such a transducer will transfer all of the energy on the largest mass to the smallest mass. However, to achieve full energy transfer in the torsional transducer, a variable mass ratio must be used. Through simulations of our 25 kg prototype antenna, we found that full energy transfer would be achieved for the following mass ratios: $m_1/m_0=0.02$; $m_2/m_1=0.005$, and certain values of the physical dimensions. Table II gives the parameters of the transducer we fabricated and the theoretically optimized version of the transducer and Fig. 8 shows the transient response for the optimized transducer. Although full energy transfer can be achieved with different mass ratios, we chose this configuration to optimize mechanical gain (178 as compared to 50) at the expense of a slightly longer energy transfer time.

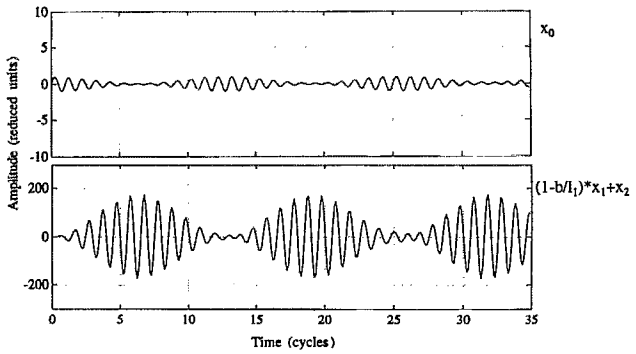

FIG. 8. Predicted transient response of the optimized three-mode antenna with two-stage torsional transducer. The mechanical amplification factor is 178 and the energy transfer time is ~5.5 oscillation cycles.

To compare a three-mode gravitational wave antenna composed of a bar and two stage optimized torsional transducer to a three-mode gravitational wave detector composed of a bar and an optimized two-mode linear transducer we employed the model of the linear system, Eq. (3), with the mass ratios of the successive stages chosen to give the same mechanical amplification of 178 as the torsional transducer. In Fig. 9 we plot the transient response of the linear system which gives the same mechanical amplification as the optimized torsional system. The rise time is 32% faster for the torsional transducer than for the linear transducer. Since the maximum bandwidth is inversely proportional to the rise time, a significantly larger bandwidth is attainable with a torsional transducer while maintaining the same mechanical amplification as a linear transducer.

The key issue in comparing various mechanical configurations is the sensitivity of a gravitational wave detector for given transducer electrical parameters. Antenna sensitivity is well described by the equivalent strain spectrum $h_{eq}(f)$, which has units of strain/(Hz)$^{1/2}$. It is defined as the square root of the fictitious strain noise spectral density needed to mimic the noise present in the antenna.[9] To calculate $h_{eq}(f)$ we first Fourier transform the equations of motion including thermal, transducer back action, and transducer additive noise sources. We then solve for the output quantity and then

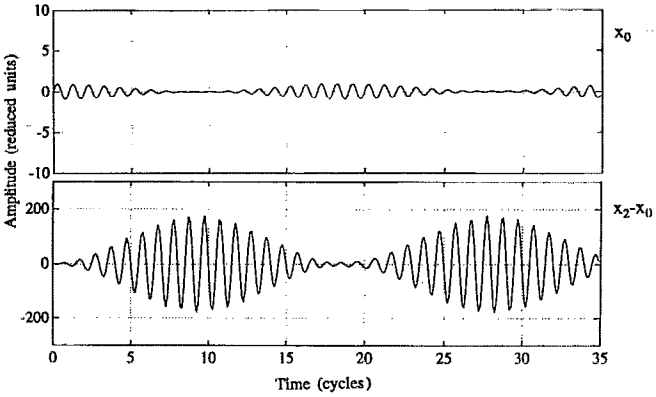

FIG. 9. Predicted transient response of the three-mode antenna with two-stage linear transducer. The mechanical amplification factor is 178 and the energy transfer time is ~9.5 oscillation cycles.

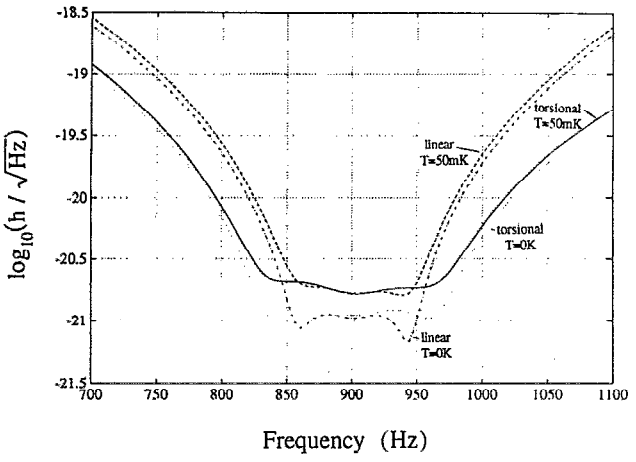

FIG. 10. Plots of $h_{eq}(f)$ for the torsional and linear transducers at $T=0$ and $T=50$ mK. For the torsional transducer at $T=0$ and $r_n=0.5$ we have $N_n=1$, and at $T=50$ mK and $r_n=0.4$ we compute $N_n=2.45$. For the linear transducer at $T=0$ and $r_n=0.4$ we have $N_n=1$, and at $T=50$ mK and $r_n=0.3$ we find $N_n=3.19$.

divide by the system transfer function to refer the noisy output signal back to an equivalent gravitational wave strain.

The thermal noise has a double-sided spectral density $S_i=2k_bTh_i$, where h_i is the damping constant of the ith mechanical resonator given by

$$h_0=m_0\omega_0/Q_0,$$
$$h_1=(m_{1u}u_1^2+m_{1l}l^2)\omega_1/Q_1, \tag{4}$$
$$h_2=(m_{2u}u_1^2+m_{2l}l^2)\omega_2/Q_2.$$

We define the transducer back action and transducer additive noise spectral densities in terms of the transducer noise N and the noise resistance r_n,

$$S_{fa}=\hbar N\omega_1 r_n; \quad S_{fb}=\hbar N/\omega_1 r_n. \tag{5}$$

In our calculations, we set $N=1$ (quantum limited transducer) and iterated through values of r_n to achieve a maximally flat $h_{eq}(f)$ curve. Figure 10 is a plot of the h_{eq} curves for the torsional and linear systems at $T=0$ K and $T=50$ mK. We also calculated the burst noise number, $N_n=p_0^2/2\hbar m_1\omega_1$ for both systems, where p_0 is the minimum detectable impulse, i.e., the impulse strength which gives a signal-to-noise ratio in the filtered output of unity. This was done by first calculating the maximum signal-to-noise ratio, given by

$$\left[\frac{S}{N}\right]^2=\frac{1}{2\pi}\int_{-\infty}^{\infty}\frac{|(1-b/l_1)x_2(\omega)+x_3(\omega)|^2}{S_n}\,d\omega, \tag{6}$$

where S_n is the output signal noise spectral density. We then set $(S/N)^2$ equal to unity and solved for p_0 from which we can calculate N_n. For $T=0$ the burst noise number for the torsional transducer as well as for the linear transducer is unity. At $T=50$ mK, for the torsional transducer $N_n=2.45$ and for the linear transducer $N_n=3.19$ so the torsional transducer is about 25% more sensitive for burst detection.

It is possible to vary the mass and dimensions of the torsional resonators to achieve either maximum bandwidth or maximum mechanical amplification. Using our simulation

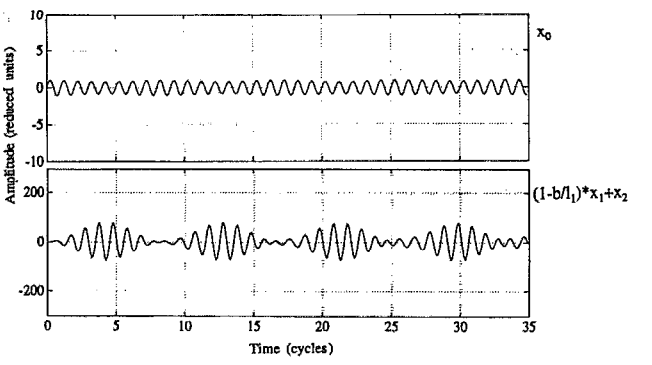

FIG. 11. Predicted transient response for the torsional transducer with maximum bandwidth. The rise time is 3.5 oscillation cycles and the mechanical amplification factor is 83.

tool, we found that if maximum bandwidth is the most important criterion for an antenna, then mechanical gain must be sacrificed, see Fig. 11. Likewise, one must sacrifice bandwidth if maximum mechanical gain is required, see Fig. 12. The mass ratios for the maximum bandwidth and maximum amplification transducers simulated in Figs. 11 and 12 are respectively;

Maximum bandwidth: $m_1/m_0=0.01$, $m_2/m_1=0.02$,

Maximum mechanical gain:

$$m_1/m_0=0.0025, \quad m_2/m_1=0.005.$$

We can see in Figs. 11 and 12, that in either case we no longer have the full transfer of energy from the largest to the smallest mass, note that the displacement of the large mass never goes to zero. It is interesting to note the effect of less than full energy transfer on the sensitivity of the antenna. Figure 13 shows plots of $h_{eq}(f)$ for a 1000 kg resonant bar antenna at $T=50$ mK equipped with a two-mode torsional transducer configured in the following cases: (1) To allow full energy transfer ($N_n=2.44$), (2) to have maximum bandwidth ($N_n=3.73$), and (3) to have maximum mechanical gain ($N_n=6.07$). We note that the lowest noise number is achieved for the case of maximum energy transfer.

Finally, as we showed in Sec. III, the torsional transducer is dynamically inequivalent to a linear spring trans-

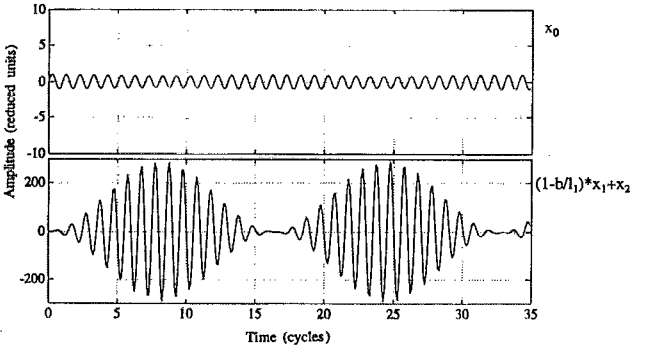

FIG. 12. Predicted transient response for the torsional transducer with maximum mechanical amplification. The rise time is 7.5 oscillation cycles and the mechanical amplification factor is 290.

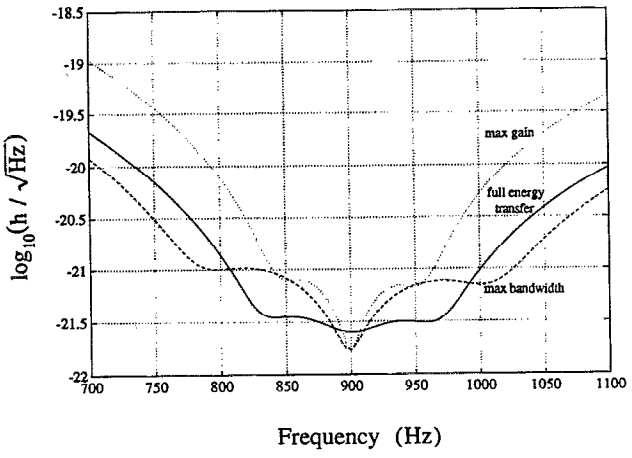

FIG. 13. Plots of $h_{eq}(f)$ for the transducer configured for either full energy transfer, maximum bandwidth, or maximum mechanical amplification. The bar mass is 1000 kg and $T=50$ mK. For the case of full energy transfer, $r_n=17$ and $N_n=2.44$; for the maximum bandwidth case, $r_n=20$ and $N_n=3.73$; and for the case of maximum mechanical amplification, $r_n=0.5$ and $N_n=6.07$.

ducer. In particular, the coupling from one stage to the next in the torsional transducer is due to the mutual acceleration of the stages, not their mutual displacements as in the linear spring transducer. Even though there exists this significant dynamical difference, the results of this section show that the performance of the two types of transducers is qualitatively much the same. However, there are subtle differences and a slight sensitivity advantage in favor of the torsional transducer which, combined with the simplicity of its fabrication make the torsional transducer an attractive alternative to conventional gravitational wave antenna transducer designs.

ACKNOWLEDGMENTS

We thank Dr. Michael A. Fisher and Dr. Roberto Onofrio for contributions to the early stages of this work. This work was supported by the National Science Foundation under Grant No. PHY-91-02164.

[1] E. Amaldi and G. Pizzella, *Relativity, Quanta and Cosmology in the Development of Scientific Thought of Einstein* **1**, 9 (1979).
[2] S. P. Boughn, W. M. Fairbank, R. P. Giffard, J. N. Hollenhorst, E. R. Mapoles, M. S. McAshan, P. F. Michelson, H. J. Paik, and R. C. Taber, Astrophys. J. **261**, L19 (1982).
[3] E. Amaldi *et al.* in *Fifth Marcel Grossman Meeting, Proceedings, Perth, Australia 1988*, edited by D. G. Blair and M. J. Buckingham (World Scientific, Singapore, 1989), p. 1691.
[4] J. C. Price, Phys. Rev. D **36**, 3555 (1987).
[5] N. Solomonson, W. W. Jonson, and W. O. Hamilton, Phys. Rev. D **46**, 2299 (1992).
[6] J. P. Richard, Phys. Rev. Lett. **52**, 165 (1984).
[7] M. Bassan, Phys. Rev. D **38**, 2327 (1988).
[8] Y. Pang and J.-P. Richard, Rev. Sci. Instrum. **63**, 56 (1992).
[9] W. W. Johnson and S. M. Merkowitz, Phys. Rev. Lett. **70**, 2367 (1993).